Center for Environmentally Sustainable in Cold Climates

Bio-Based Renewable Additives for Anti-Icing Applications (Phase II)

Mehdi Honarvar Nazari, Taekil Oh, Alexander Charlemagne Ewing, Deborah Ave Okon, Yan Zhang, Brandon Avalos, Eisa Alnuaimi, Eden Adele Havens, Xianming Shi

Department of Civil and Environmental Engineering
Washington State University

Date: 07/01/2018

Prepared by:

Center for Environmentally Sustainable Transportation in Cold Climates
Duckering Building, Room 245
P.O. Box 755900
Fairbanks, AK 99775

U.S. Department of Transportation
1200 New Jersey Avenue, SE
Washington, DC 20590

INE/AUTC 18.13

REPORT DOCUMENTATION PAGE			Form approved OMB No.
Public reporting for this collection of information is estimated to average 1 hour per response, including the time for reviewing instructions, searching existing data sources, gathering and maintaining the data needed, and completing and reviewing the collection of information. Send comments regarding this burden estimate or any other aspect of this collection of information, including suggestion for reducing this burden to Washington Headquarters Services, Directorate for Information Operations and Reports, 1215 Jefferson Davis Highway, Suite 1204, Arlington, VA 22202-4302, and to the Office of Management and Budget, Paperwork Reduction Project (0704-1833), Washington, DC 20503			
1. AGENCY USE ONLY (LEAVE BLANK)	2. REPORT DATE 01/2019	3. REPORT TYPE AND DATES COVERED Final Report: 9/2016 – 12/2018	
4. TITLE AND SUBTITLE Bio-Based Renewable Additives for Anti-Icing Applications (Phase II)			5. FUNDING NUMBERS
6. AUTHOR(S) Mehdi Honarvar Nazari, Ph.D., Washington State University Taekil Oh, Washington State University Alexander Charlemagne Ewing, Washington State University Deborah Ave Okon, Washington State University Yan Zhang, M.Sc. Washington State University Brandon Avalos, Washington State University Eisa Alnuaimi, Washington State University Eden Adele Havens, Washington State University Xianming Shi, Ph.D., P.E., Washington State University			
7. PERFORMING ORGANIZATION NAME(S) AND ADDRESS(ES) Laboratory of Corrosion Science & Electrochemical Engineering Department of Civil & Environmental Engineering, P.O. Box 642910 Washington State University, Pullman, WA 99164-2910			8. PERFORMING ORGANIZATION REPORT NUMBER INE/AUTC 18.13
9. SPONSORING/MONITORING AGENCY NAME(S) AND ADDRESS(ES) Center for Environmentally Sustainable Transportation in Cold Climates University of Alaska Fairbanks, Duckering Building, Room 245, P.O. Box 755900, Fairbanks, AK 99775-5900 U.S. Department of Transportation, 1200 New Jersey Avenue, SE Washington, DC 20590			10. SPONSORING/MONITORING AGENCY REPORT NUMBER
11. SUPPLENMENTARY NOTES			
12a. DISTRIBUTION / AVAILABILITY STATEMENT: No restrictions			12b. DISTRIBUTION CODE
13. ABSTRACT: The performance and impacts of several agro-based anti-icers along with a traditional chloride-based anti-icer (salt brine) were evaluated. A statistical design of experiments (central composite design) was employed for developing anti-icing liquids consisting of cost-competitive chemicals such as agro-based compounds (e.g., Concord grape extract and glycerin), sodium chloride, sodium metasilicate, and sodium formate. The following experimentally obtained parameters were examined as a function of the formulation design: ice-melting capacity at 25°F (−3.9°C), splitting strength of Portland cement mortar samples after 10 freeze-thaw/deicer cycles, corrosion rate of C1010 carbon steel after 24-hour immersion, and impact on asphalt binder stiffness and *m*-value. One viable formula ("best performer") was tested for thermal properties by measuring its differential scanning calorimetry (DSC) thermograms, the friction coefficient of asphalt pavement treated by this anti-icing formulation (vs. 23 wt.% NaCl and beet juice blend) at 25°F after being applied at 30 gallons per lane mile (1 hour after simulated trafficking and plowing), and other properties (pH, oxygen demand in COD). Laboratory data shed light on the selection and formulation of innovative agro-based snow- and ice-control chemicals that can significantly reduce the costs of winter maintenance operations.			
14- KEYWORDS: Agro-based anti-icer; ice-melting performance; Portland cement mortar; splitting strength; asphalt binder; stiffness; *m*-value; corrosivity; DSC; friction coefficient; COD			15. NUMBER OF PAGES: 42 16. PRICE CODE: N/A
17. SECURITY CLASSIFICATION OF REPORT Unclassified	18. SECURITY CLASSIFICATION OF THIS PAGE Unclassified	19. SECURITY CLASSIFICATION OF ABSTRACT Unclassified	20. LIMITATION OF ABSTRACT N/A

NSN 7540-01-280-5500

STANDARD FORM 298 (Rev. 2-98) Prescribed by ANSI Std. 239-18 298-

Disclaimer

This document is disseminated under the sponsorship of the U.S. Department of Transportation in the interest of information exchange. The U.S. Government assumes no liability for the use of the information contained in this document. The U.S. Government does not endorse products or manufacturers. Trademarks or manufacturers' names appear in this report only because they are considered essential to the objective of the document. Opinions and conclusions expressed or implied in the report are those of the author(s). They are not necessarily those of the funding agencies.

METRIC (SI*) CONVERSION FACTORS

APPROXIMATE CONVERSIONS TO SI UNITS

Symbol	When You Know	Multiply By	To Find	Symbol
		LENGTH		
in	inches	25.4		mm
ft	feet	0.3048		m
yd	yards	0.914		m
mi	Miles (statute)	1.61		km
		AREA		
in^2	square inches	645.2	millimeters squared	cm^2
ft^2	square feet	0.0929	meters squared	m^2
yd^2	square yards	0.836	meters squared	m^2
mi^2	square miles	2.59	kilometers squared	km^2
ac	acres	0.4046	hectares	ha
		MASS (weight)		
oz	Ounces (avdp)	28.35	grams	g
lb	Pounds (avdp)	0.454	kilograms	kg
T	Short tons (2000 lb)	0.907	megagrams	mg
		VOLUME		
fl oz	fluid ounces (US)	29.57	milliliters	mL
gal	Gallons (liq)	3.785	liters	liters
ft^3	cubic feet	0.0283	meters cubed	m^3
yd^3	cubic yards	0.765	meters cubed	m^3
Note: Volumes greater than 1000 L shall be shown in m^3				
		TEMPERATURE (exact)		
ºF	Fahrenheit temperature	5/9 (ºF-32)	Celsius temperature	ºC
		FORCE and PRESSURE or STRESS		
lbf	pound-force	4.45	newtons	N
psi	pound-force per square inch	6.89	kilopascals	kPa

These factors conform to the requirement of FHWA Order 5190.1A *SI is the symbol for the International System of Measurements

APPROXIMATE CONVERSIONS FROM SI UNITS

Symbol	When You Know	Multiply By	To Find	Symbol
		LENGTH		
mm	millimeters	0.039	inches	in
m	meters	3.28	feet	ft
m	meters	1.09	yards	yd
km	kilometers	0.621	Miles (statute)	mi
		AREA		
mm^2	millimeters squared	0.0016	square inches	in^2
m^2	meters squared	10.764	square feet	ft^2
m^2	meters squared	1.196	square yards	yd^2
km^2	kilometers squared	0.39	square miles	mi^2
ha	hectares (10,000 m^2)	2.471	acres	ac
		MASS (weight)		
g	grams	0.0353	ounces (avdp)	oz
kg	kilograms	2.205	pounds (avdp)	lb
mg	megagrams (1000 kg)	1.103	short tons	T
		VOLUME		
mL	milliliters	0.034	fluid ounces (US)	fl oz
liters		0.264	gallons (liq)	gal
m^3	meters cubed	35.315	cubic feet	ft^3
m^3	meters cubed	1.308	cubic yards	yd^3
		TEMPERATURE (exact)		
ºC	Celsius temperature	9/5 ºC+32	Fahrenheit temperature	ºF
		FORCE and PRESSURE or STRESS		
N	newtons	0.225	pound-force	lbf
kPa	kilopascals	0.145	pound-force per square inch	psi

Acknowledgments

The authors acknowledge the financial support provided by the Center for Environmentally Sustainable Transportation in Cold Climates, Dr. Balasingam Muhunthan at the Washington Center for Asphalt Technology for providing lab access to run most of the bending beam rheometer (BBR) tests, the National Center for Asphalt Technology for running the rest of the BBR tests, Dr. Somayeh Nassiri for providing lab access to run the ice-melting test, Dr. Junna Xin for providing lab access to run the differential scanning calorimetry test, Natalia Kaiser for providing lab access to run the chemical oxygen demand test, Dr. Daniel J. Dolan for providing lab access to run the splitting strength test, and Montana State University for providing lab access to run the friction test on deiced and anti-iced pavement. The authors would also like to thank Michelle Akin, Sen Du, and Yan Zhang.

Table of Contents

List of Figures

List of Tables

Executive Summary

Road maintenance agencies are continually challenged in providing a high level of service on roadways and improving safety and mobility in a cost-effective manner while minimizing adverse effects to the environment. Large amounts of liquid chemicals, known as anti-icers, are applied on roadways during winter to keep them clear of ice and snow. These anti-icers are mainly chloride-based salts that do not degrade once used and thus pose significant environmental risk over time. About 27 million tons of chloride-based salts is used annually in the United States for snow- and ice-control purposes. Maintenance agencies are constantly seeking an alternative to chloride-based deicing salts, one with maximum anti-icing efficiency and minimum drawbacks.

In recent decades, agro-based chemicals such as desugared beet molasses and glycerin (glycerol) have been introduced in snow- and ice-control operations, used alone or more commonly used as additives for chloride-based products. Agro-based chemicals are produced by fermentation and processing of beet juice, molasses, corn, and other agricultural products. The deicer formulation is noncorrosive, inexpensive, water soluble, and readily available in large quantities. Agro-based additives provide enhanced ice-melting capacity, reduce deicer corrosivity, and remain effective on roadways longer than standard chemicals.

Through this project, the research team has developed an innovative high-performance "green" anti-icer that can minimize the impacts of traditional chloride-based salts on concrete, asphalt, and metallic components. Selected constituent materials in this anti-icer pose minimal toxicity to the environment (e.g., no heavy metal content) and are derived from eco-friendly cost-effective processes. Agro-based solutions derived from locally sourced agro-based materials mixed with salt brine and commercial additives (with little toxicity) have been tested for ice-melting capacity, ability to protect asphalt binder and concrete, effect on the friction coefficient of

iced asphalt pavement, and anti-corrosion performance. The main criterion for choosing the best-performing anti-icer was ice-melting capacity. This research contributes to the knowledge base relevant to agro-based anti-icers and introduces a new class of high-performance “green” anti-icers.

CHAPTER 1.0 INTRODUCTION

1.1 Problem Statement

The environmental cost associated with using snow- and ice-control products should be in line with the value they provide. Sustainability principles must be considered in the winter maintenance of highways. Compared with deicing and sanding, anti-icing of roadways leads to improved levels of service, reduced need for chemicals, cost saving, safety, and increased mobility (Conger 2005, Staples et al. 2004). However, there are concerns over anti-icers available on the market: their damage to metal (chlorides), impact on concrete and asphalt (acetates), toxicity to aquatic resources (oxygen depletion), etc. Many agencies are looking for ways to maximize the benefits of agro-based products and minimize their drawbacks. Based on earlier research by the authors, further research was needed on the value-added utilization of locally sourced agro-based extracts.

1.2 Background

The U.S. is currently spending about $2.3 billion annually for winter maintenance operations; the damage caused by deicers to infrastructure and the environment adds at least $5 billion (Fay et al. 2013). Winter maintenance agencies have been faced with many challenges: increased traffic demands, higher customer expectations, and unprecedented staffing and funding constraints (Fay et al. 2013, Li et al. 2013, Shi et al. 2013). A study showed that the Nevada Department of Transportation (NDOT) has spent about $12.8 million on road maintenance operations during winter season 2006–07 (Ye et al. 2009). Use of updated weather information enabled more proactive strategies for snow and ice control, which resulted in a savings of about $0.6 million per season (Ye et al. 2009).

Chloride salts persist in the environment and pose a significant risk over time (Fay et al. 2014). Currently, 24.5 million metric tons (27 million U.S. tons) of sodium chloride salt is used in the U.S. for snow and ice control on roadways, costing about $1.18 billion (Lilek 2017). Glycerol (also known as glycerin), which is a by-product of biodiesel or triglyceride processing, has been used widely in anti-icing fluids (Johnson 2017, Sapienza et al. 2012, Simmons et al. 2007). Taylor et al. (2010) examined the brines made of glycerol, NaCl, $MgCl_2$, and commercial deicers, individually or in combination, and concluded that a blend of 4:1 of glycerol/NaCl performs best and has low negative impacts. This blend is highly viscous. Dilution of the blend allows anti-icing application, but can undermine the blend's effectiveness. Furthermore, use of glycerol poses potential risk to water quality, which has to be mitigated by limiting the amount of glycerol in the formulation to control contaminants. Glycerol merits more research to explore the synergy of it and other additives in optimizing liquid product formulations. Desugared molasses, a by-product of the beet sugar refining process, is readily available at low cost and has been disclosed as an effective user-friendly and environmentally friendly ingredient for anti-icing, deicing, or pre-wetting operations (Bloomer 2002, Ossian and Behrens 2009).

1.3 Objectives

The objective of this exploratory study was to develop innovative anti-icing formulations for snow and ice control on highways by using beet sugar refining by-products and other bio-based additives. These formulations are expected to have improved ice-melting and corrosion-inhibiting capacity, with less impact on the durability of concrete and asphalt binder.

1.4 Expected Benefits

This project fits the research thrust of the Center for Environmentally Sustainable Transportation in Cold Climates (CESTiCC): "*reducing environmental impacts during*

construction, operations and preservation through effective design, management and preservation strategies." This project also meets the U.S. Department of Transportation's (USDOT) strategic goal in environmental sustainability, as it helps "*advance environmentally sustainable policies and investments that reduce harmful emissions from transportation sources."* Development of alternative anti-icing products serves the public interest. As such, research is expected to generate significant cost savings for departments of transportation and other maintenance agencies, traveler benefits in terms of improved safety and mobility, and societal benefits by *reducing the amount of chlorides in the environment*.

The findings from this work will provide maintenance agencies with more options in their snow- and ice-control toolbox for sustainable winter road service. The exploration of bio-based renewable additives for anti-icing applications will also add value to *agricultural by-products and stimulate local economies.*

CHAPTER 2.0 METHODOLOGY

2.1 Research Approach

The objective of this research was to develop anti-icing liquids consisting of cost-competitive chemicals (e.g., desugared beet molasses), sodium chloride, and other additives (e.g., bio-derived succinate salts, thickeners, concrete protection additives, and corrosion inhibitors). The optimized addition of renewable bio-based additives to salt brine enhances its anti-icing and deicing performance at cold temperatures, similar to the effect of $MgCl_2$, at reasonable cost, while producing substantial savings through reduced application rates, reduced corrosion to metals, and reduced impact on concrete or asphalt materials. The research team developed several liquid products tailored to meet the varying requirements in highway anti-icing performance, cost, and impacts. The team also addressed current gaps in the development of "green" anti-icers, that is, the synergy between various additives.

2.2 Work Plan – Task Descriptions and Milestones

2.2.1 Identify and Evaluate Individual "Green" Additives

The identification of "green" additives has mostly been built on the success of previous research by the principal investigator of this project. Patents and other published literature were examined to understand recent research on the topic and identify active ingredients and additives for eco-friendly liquid formulations. This step is an essential part of a mass customization strategy that requires modular product design. The constituent materials selected should pose minimal toxicity to the environment (e.g., with low nitrogen, phosphate, and heavy metal content), and those that come from eco-friendly cost-effective processes are preferred. Mixed with 23% salt brine, locally sourced agro-based materials (with or without further treatment) and commercial

additives with little toxicity were tested for their potential in terms of improved ice-melting and corrosion-inhibiting capacity and reduced impact on asphalt binder and concrete material. Before this step, we optimized the process of preparing agro-based materials using different locally sourced fruit wastes and changing the synthesis parameters. This step will be explained in more detail in Section 2.2.3 Systematic Laboratory Investigation and Formulation Optimization – Preparation of the plant extract.

2.2.2 Statistical Design of Experiments

In order to minimize the number of experiments needed to explore a large domain of unknown factors and interactions, we used a scheme of statistical design of experiments known as central composite design. For instance, if we planned to investigate four influential factors, each varying at five different levels, without experimental design, there would be a total of $4^4 = 256$ experiments. With central composite design, however, one could choose to conduct only 21 experiments, the data from which should be sufficient to reasonably illustrate the inherent relations between the influential factors and the target factors.

Using central composite design, we chose four factors of X_1, X_2, X_3, and X_4 as the weight percent of Concord grape extract, glycerol, sodium formate, and sodium metasilicate, respectively. The weight percent range of 0–6 g was chosen for X_1–X_3, and 0–4.5 g for X_4. The anti-icer formulations were investigated by adopting the design parameters and associated target attributes, shown in Table 2.1.

Table 2.1 Anti-icer mixtures designed based on central composite design method using Design-Expert® software

Mix #	**Weight percent of additives (%)**			
	Concord grape extract	**Glycerol**	**Sodium formate**	**Sodium metasilicate**
Mix 1	2.40	2.40	2.40	1.80
Mix 2	4.80	2.40	2.40	1.80
Mix 3	2.40	2.40	2.40	1.80
Mix 4	1.94	2.86	1.94	2.14

Mix #	Weight percent of additives (%)			
	Concord grape extract	**Glycerol**	**Sodium formate**	**Sodium metasilicate**
Mix 5	1.94	2.86	2.86	2.14
Mix 6	2.40	2.40	2.40	1.80
Mix 7	2.40	2.40	2.40	1.80
Mix 8	2.40	2.40	4.80	1.80
Mix 9	1.94	1.94	1.94	1.46
Mix 10	1.94	1.94	2.86	1.46
Mix 11	2.86	1.94	1.94	2.14
Mix 12	2.86	2.86	2.86	1.46
Mix 13	2.40	2.40	2.40	3.60
Mix 14	2.86	2.86	1.94	1.46
Mix 15	2.40	4.80	2.40	1.80
Mix 16	2.40	2.40	2.40	0.00
Mix 17	2.40	0.00	2.40	1.80
Mix 18	2.40	2.40	0.00	1.80
Mix 19	2.86	1.94	2.86	2.14
Mix 20	0.00	2.40	2.40	1.80
Mix 21	2.40	2.40	2.40	1.80

2.2.1 Systematic Laboratory Investigation and Formulation Optimization

Following the established experimental design, several measures were used for screening tests on promising liquid formulations. To prepare the anti-icer formulations, we used deionized water, reagent-grade sodium chloride, sodium metasilicate, and sodium formate, commercial-grade glycerin, and laboratory developed Concord grape extract. Each formulation had the same amount of sodium chloride (18.4 wt.%) and various amounts of other constituents, as shown in Table 2.1.

Preparation of the plant extract

For preparation of the plant extract, the as-received Concord grape waste powder was milled to get a more homogenous powder. Then, 30 g of the powder was chosen for chemical and biological degradation. For chemical degradation, 30 g of the Concord grape powder, 120 g of urea, 0.5 g of $Ca(OH)_2$, and 3 g of NaOH were added to 200 mL of deionized water (stage A). The

solution was stirred vigorously for 30 min, then placed in the refrigerator at -20°C overnight. The iced solution was removed from the refrigerator and put in room temperature for some hours until a slurry of ice and liquid was achieved. The solution was then stirred vigorously for 30 min, during which 250 mL of water was added gradually (stage B). For biological degradation, the pH of the prepared solution was adjusted to around 8.5 by adding HNO_3 and NaOH. A mixture of KH_2PO_4, $NaH_2PO_4.H_2O$, and $MgSO_4.7H_2O$ with the molar ratios of 7, 10.7, and 1, respectively, and total weight of less than 4 g was added to the solution to create an appropriate environment for the growth of bacteria. Next, 100 mL of *Bacillus megaterium* bacteria (NRRL B-14308) was added to the solution, and the solution was put in the shaker for 21 days to complete the biodegradation process (stage C).

Before choosing Concord grape (fiber) waste to make the fruit extract, different fruit wastes including apple pomace, apple fiber, cherry pomace, Concord grape fiber, blueberry fiber, orange peels, and potato peels were examined. Among them, Concord grape fiber extract showed the most promise in terms of ice-melting capacity at 15°F and 25°F and corrosion inhibition efficiency for C1010 carbon steel in NaCl solution. In addition, three variations of the process were explored to enhance the performance of the end product. For this purpose, in stage A, two different amounts of NaOH were used: 4 g and 3 g. In stage B, two different volumes of deionized water were used: 500 mL and 250 mL. In stage C, two different periods of biochemical degradation were used: 14 days and 21 days. Finally, we chose to use 3g NaCl in stage A, 250 mL of water in stage B, and 21 days of biochemical degradation process in stage C.

Freeze-thaw test

The effects of anti-icers on concrete were assessed by conducting a freeze-thaw test of Portland cement mortar (PCM) samples in the presence of anti-icers, following the SHRP

(Strategic Highway Research Program) H205.8 test method with minor modifications. The test evaluates the combined effects of liquid chemicals and freeze-thaw cycling on the structural integrity of specimens of non-air-entrained mortar. Mortar samples were prepared in 5.1 cm × 10.2 cm (2 in.: diameter × 4 in.: length) poly (vinyl chloride) piping with a volume of 52.5 cm^3. The mortar mix design had a water-to-cement ratio of 0:5, sand-to-cement ratio of 3:1, and water reducer of 1.5 mL. The cement used was Portland cement type I-II; the sand used was Sakrete multipurpose. Samples were cured in water for the first 24 h before being placed in a container with 100% relative humidity. The dry weight of each sample at 28 days was recorded before the sample was placed on a sponge inside a dish containing 310 mL of diluted (3%) anti-icer solution. The dish was covered in plastic wrap to press the mortar samples into the sponge and to prevent evaporation of anti-icer solutions. Three mortar specimens were tested in each anti-icer solution. 23% NaCl brine solution and beet juice blend (80% (v/v) 23% NaCl solution + 20% (v/v) beet juice) were used as the controls. A thermocouple was embedded in one of the control mortar samples to monitor temperatures during freeze-thaw cycling. The sealed dishes were placed in the freezer for 16 to 18 h, at -20.8 ± 0.2°C (-5.44 ± 0.4°F), and afterward were placed in a laboratory environment for 6 to 8 h, at 23.2 ± 0.2°C (73.8 ± 0.4°F). The cooling rate in the freezer and the heating rate in the laboratory environment were about 0.06°C/min and 0.07°C/min, respectively. This cycle was repeated for 10 days. The test specimens were removed from the dish, and the scaled-off materials were removed using a plastic brush. The specimens were air-dried overnight before the final weight of each was recorded. Most of the samples showed weight gain in spite of scaling, which demonstrates the absorption of anti-icers by most of the specimens. Therefore, weight loss data were not used for evaluating the effectiveness of the anti-icer solutions.

Ice-melting test

The SHRP ice-melting test (H-205.1 and H-205.2) measures the amount of ice melted by deicers over time. In this test, liquid or solid deicers are uniformly spread over the prepared ice, and the melted liquid is removed for volume measurements (Chappelow et al. 1992). A modified SHRP test using 1.4 mL anti-icer, 48 mL distilled deionized water, and a 150 × 20 mm (5.9 in.: diameter × 0.8 in.: depth) polystyrene petri dish was conducted to measure the ice-melting capacity of the anti-icer at -9.4°C (15°F). The anti-icer was applied evenly over the ice surface with a syringe. After 10, 20, 30, 45, and 60 min, the liquid volume was removed and volumetrically measured with a calibrated syringe. Another parallel series of tests were conducted in a 3.65 m × 4.27 m state-of-the-art temperature-regulated environmental chamber, following the same procedure. The tests were conducted at -3.9°C (25°F). To ensure statistical reliability, duplicate tests were performed for each combination of anti-icer type.

Low-temperature behavior of asphalt binder

A customized test protocol was used to assess the effect of anti-icers on the low-temperature behavior of asphalt binder. A bending beam rheometer (BBR) was used for this purpose. Asphalt binder (PG 64-28 from Western States Asphalt, Inc.) was first aged in a rolling thin-film oven to simulate the effects of hot-mix asphalt concrete. The asphalt binder was then placed in a pressure aging vessel for 20 h to simulate 5–10 years of in-service aging. The asphalt binders were moved to a can, and 4 mL of anti-icer solution was applied for each 40 g of binder, after which the cans were put in an oven at 80°C for 1 h, followed by 2 h at 155°C and atmospheric pressure. Finally, beams were molded and tested in the BBR.

Corrosion behavior

The corrosion caused by anti-icers to C1010 carbon steel (ASTM A569) was assessed using the linear polarization resistance (LPR) technique. Measurements for this technique were carried out in a PARSTAT-MC multichannel potentiostat-galvanostat, coupled with a three-electrode electrochemical cell for each channel. Before testing, the steel coupons were wet-polished using 60 to 1500 grit silicon carbide papers, and washed with ethanol and distilled deionized water. For each anti-icer, at least two steel coupons were exposed to anti-icer for 24 h. The LPR measurement "is the only corrosion monitoring method that allows corrosion rates to be measured directly, in real time" (Metal Samples 2018). This electrochemical technique provides an alternative to the gravimetric method in rapidly assessing the corrosivity of solutions. The corrosivity of each anti-icer was reported as milli-inches per year (mpy).

DSC thermogram test

The DSC (differential scanning calorimetry) thermogram test is a laboratory method used to quantify deicer performance. The test measures the energy necessary to maintain a near-zero temperature difference between the test substance (deicer) and an inert reference material, with the two subjected to an identical temperature program. The heat-flow measurements indicate phase transitions, energy changes, and kinetics. The DSC measurement used in this research required 5–10 mg of the sample, which was sealed in an aluminum capsule.

pH measurements

The pH of samples was measured using a Milwaukee MW100 portable pH meter with 0.1 pH resolution.

COD measurements

The best-performer sample and beet juice blend were used for the COD (chemical oxygen demand) test. Both solutions were diluted to a ratio of 1000:1 by adding deionized water. Then 2 mL of the diluted solution was added to COD Standard Solution containing potassium dichromate as a strong oxidizing agent. The mixture was heated at 150°C for 2 h. After the mixture cooled to room temperature, the mg/L COD was measured at the wavelength of 420 nm using a Gen20 spectrophotometer.

Snow–pavement bond and friction measurements

Laboratory tests to assess the performance of a few select products during a winter storm with realistic pavement, snow, and traffic simulation were conducted at the Subzero Science and Engineering Research Facility (SSERF) at Montana State University (MSU), in the Cold Structures Testing Chamber at a temperature of 25°F. The pavement samples were made at a batch plant with a 9.5 mm Superpave HMA mix design, PG 58-28 asphalt binder, and air void content of 4.2%. The pavement mix was compacted in a large wood form to 1 in. thick with a steel drum roller, without vibration (Figure 2.1, left). Samples measuring 9 in. by 19 in. were cut from the pad and "aged" by lightly abrading the pavement surface with an angle grinder to expose the aggregate and make surface roughness and texture similar for all pavement samples (Figure 2.1, right).

Figure 2.1 Pavement sample during construction (left) and after preparation (right)

Three types of tests were conducted, distinguished by when and how deicer material was applied. The tests in which no chemical was applied are referred to as the controls; the controls were used to compare the effectiveness of deicing and anti-icing with chemicals. The sequence of steps during each of the four types of tests is shown in Table 2.2. Details of each activity (applying snow, applying salt, trafficking, and measuring snow–pavement bond and friction) are described next. All pavement samples were rinsed, scrubbed and dried before being returned to the cold chamber for temperature equilibration.

Table 2.2 Sequence of steps for snow/traffic tests

Control (No Chemical)	Anti-icing	Deicing with Pre-wet Salt
1. Measure friction	1. Measure friction	1. Measure friction
	2. Apply liquid anti-icer	
2. Apply snow	3. Apply snow	2. Apply snow
3. Measure friction	4. Measure friction	3. Measure friction
		4. Apply pre-wet salt
4. Traffic	5. Traffic	5. Traffic
5. Measure friction	6. Measure friction	6. Measure friction
6. Measure snow–pavement bond	7. Measure snow–pavement bond	7. Measure snow–pavement bond
7. Measure friction	8. Measure friction	8. Measure friction

The liquid products used for these tests were

1. 23 wt.% NaCl;
2. 23 wt.% NaCl: beet juice at 80 to 20 by volume;
3. Predicted best-performing blend (BP-4 anti-icing); and
4. Formulation #3 with the “CG” removed (BP-3 anti-icing).

For anti-icing tests, the liquids were applied directly to the clean, dry pavement with a micropipette: 36 drops of 59 µl per drop spaced 2 in. apart for a total application rate of 30 gal/lane-mile. For pre-wet deicer tests, 71 µl of liquid deicer was mixed with 36 NaCl particles sieved to

minus No. 4, plus No. 8 with a mass of 2.13 g for an application rate of 250 lb/lane-mile and pre-wet rate of 8 gal/ton. The 36 pre-wet salt particles were placed 2 in. apart on compacted snow before trafficking.

Snow was made by SSERF staff in the Cold Hydrodynamics Chamber at MSU using a constructed system with a high-humidity cold-temperature chute. Snow crystals form on strings and drop into a tray. Snow was collected from the tray and stored in insulated coolers. The snow used in laboratory tests was stored for at least 4 days and not more than 4 months to ensure consistency in morphology of grain structure. For each test, 800 g of snow sieved through a 1 mm sieve was uniformly distributed on the pavement sample and compacted at 60 psi for 5 min (Figure 2.2). The loose depth of snow was about 19 mm; the compacted depth, about 13 mm. The average density of the compacted and trafficked snow was 0.0202 lb/in^2.

Figure 2.2 Snow production, sieving and compaction

To simulate vehicle traffic in the laboratory, the pavement samples were trafficked using a custom-built automated trafficking machine (Figure 2.3). Pneumatic cylinders apply load onto an axle fitted with a single tire, which presses down on the pavement samples. The load applied to the pavement samples was 730 lb. The wheel assembly is stationary and a platform containing the sample translates back and forth under the tire, causing the tire to rotate. During testing, the track moved at a speed of about 0.8 mph (1.2 ft per second). Traffic simulation occurred after snow compaction during control and anti-icing tests. During pre-wet deicer tests, traffic simulation occurred 18 min after the last salt particle was applied to the snow. The samples were trafficked for 500 single tire passes (equivalent to 250 2-axle vehicles passes of a single tire on the pavement sample), which took about 13 min.

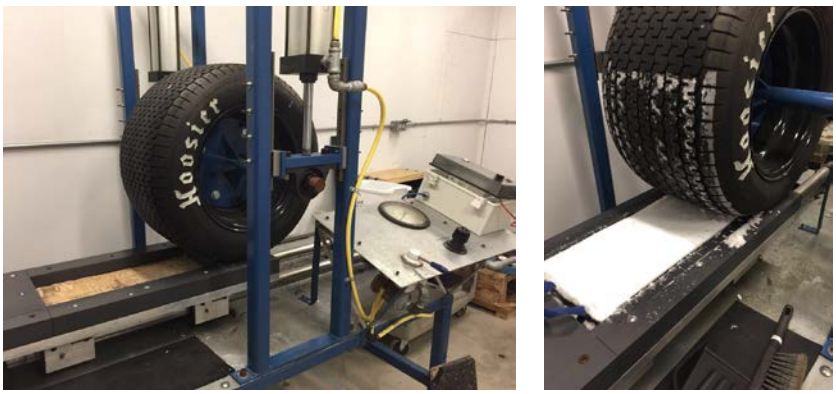

Figure 2.3 Automated trafficking machine used for simulating vehicle traffic in the laboratory

The shear force required to plow the snow from the pavement surface was measured to investigate the effect of deicing and anti-icing on the snow–pavement bond. After trafficking, individual sections of snow were isolated by cutting the snow with a serrated saw and carefully removing snow adjacent to intact 2 in. square specimens. A hollow metal box was placed around the specimen and pulled horizontally using a spring scale to measure the maximum force required to shear the snow from the pavement. The process of isolating the snow specimens for shearing and shearing the sample from the pavement is shown in Figure 2.4. Eight snow–pavement bond

shear force samples were measured during each individual test. The shear strength of the snow pavement bond is the maximum shear force divided by the contact area (1.75 in*1.75 in = 3.06 in^2).

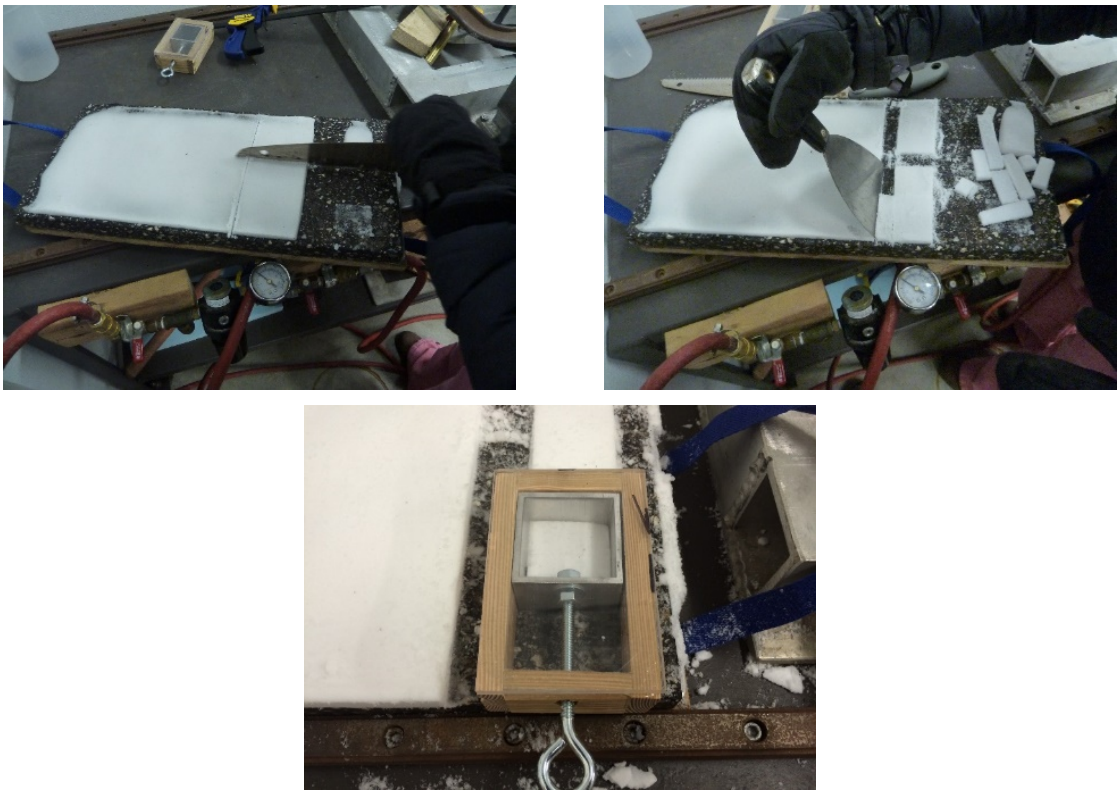

Figure 2.4 Snow production, sieving, and compaction

Surface friction on the pavement surface was measured using a static friction tester immediately after measuring the force required to shear the snow from the pavement (Figure 2.5). The static friction tester had a ¼ in. thick, 4 in. square neoprene rubber contact surface (durometer rating of 30A). The apparatus was pulled horizontally across the pavement surface at the same location as the sheared snow, and the force needed to overcome static friction was measured with a spring scale. The coefficient of static friction is defined as the ratio of the horizontal pulling force to the weight of the friction tester. Friction was measured on the pavement samples prior to each experiment on clean, dry pavement (baseline friction), on the compacted snow before trafficking

(compacted snow friction), after trafficking (trafficked snow friction), and after shearing the snow (residual friction).

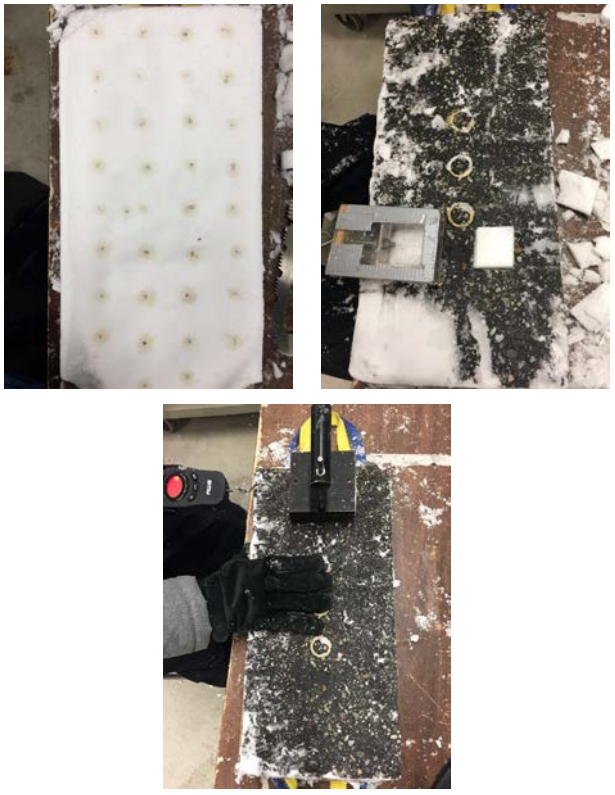

Figure 2.5 Static friction measurements

CHAPTER 3.0 RESULTS AND DISCUSSION

3.1 Ice-Melting Capacity of Anti-Icers

Figure 3.1 shows the 20 min ice-melting capacity of selected anti-icers at 25°F. The differences in ice-melting capacities of 23% NaCl and beet juice blend with mixture 20 were significant (equal or more than 0.2 mL brine/g anti-icer), which indicates the advantage of the use of mixture 20 over them. Figure 3.2 shows the 60 min ice-melting capacity of selected anti-icers at 25°F. No sample had an ice-melting capacity of at least 0.2 unit more than both 23% NaCl and beet juice blend. The best sample (sample 10) could outperform 23% NaCl by more than 0.2 unit and beet juice blend by 0.13 unit. This made it a potential candidate for using instead of 23% NaCl brine and beet juice blend as the controls. Considering ice-melting capacity at both 20 min and 60 min, only mixture 10 had a relative advantage over the controls.

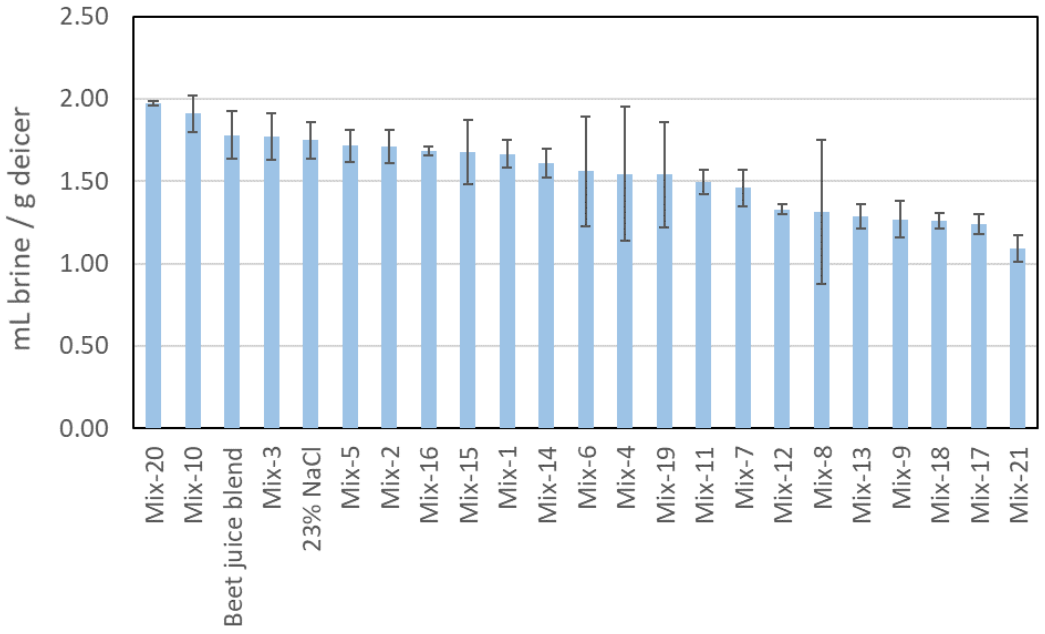

Figure 3.1 Ranking of mixtures based on ice-melting capacity after application of anti-icers at 20 min, 25°F obtained using a SHRP test method (error bars represent standard error)

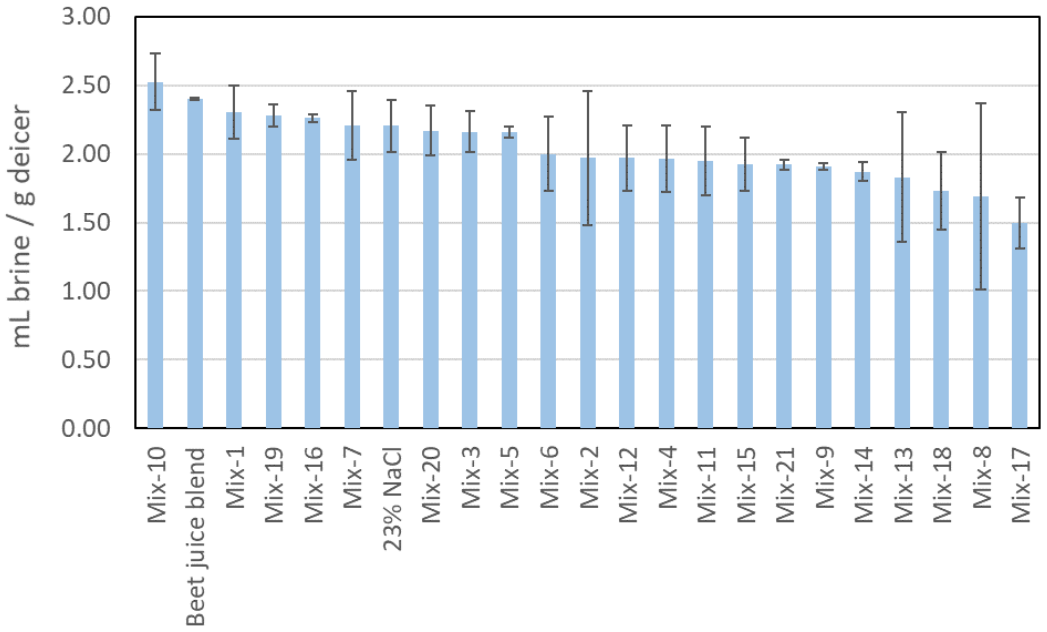

Figure 3.2 Ranking of mixtures based on ice-melting capacity after application of anti-icers at 60 min, 25°F obtained using a SHRP test method (error bars represent standard error)

3.2 Effect of Freeze-Thaw in the Presence of Anti-Icers on PCM Strength

Figure 3.3 illustrates the average splitting strength of PCM (Portland cement mortar) samples after 10-cycle freeze-thaw testing in various anti-icers, along with two control samples in 23%NaCl brine and beet juice blend. These results show that the splitting strength of the PCM samples exposed to all mixtures but mixtures 2 and 21 was higher than that of the samples exposed to 23%NaCl. Note that all samples had lower splitting strength values than the samples exposed to beet juice blend.

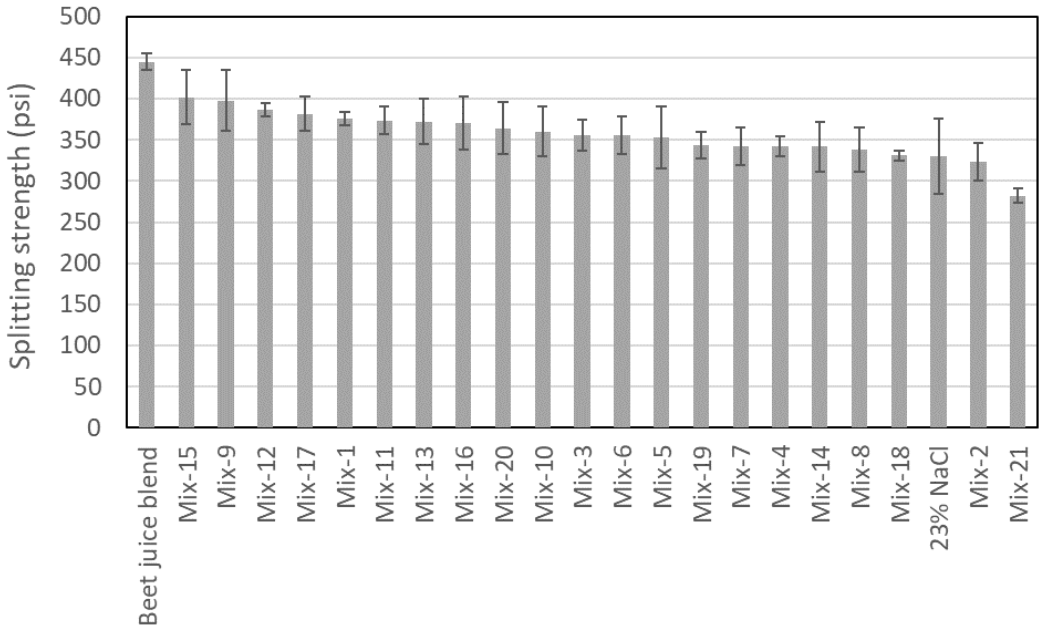

Figure 3.3 Splitting strength of mortar as a function of anti-icer type after 10-cycle freeze-thaw test (error bars represent standard error)

3.3 Impacts of Anti-Icer Mixtures on Low Temperature Behavior of Asphalt Binder

The effect of anti-icers on asphalt was assessed with a bending beam rheometer (BBR) by exposing the asphalt binder to anti-icers and thermal and pressure aging, and subsequent testing of the binder beams with the BBR. The BBR test provides values for creep stiffness and *m*-value (Figure 3.4 and Figure 3.5). Higher stiffness values correspond to higher thermal stresses, so a maximum limit of 185.13 MPa was specified. On the other hand, lower *m*-values indicate less ability to relax, so a minimum limit of about 0.271 was specified. The *m*-value and stiffness values varied, in the range of 0.271–0.406 and 112.13–185.13 MPa, respectively. In both parameters, Mix-20 has values close to the beet juice blend and salt brine. The experimental results indicated the higher impact of anti-icer design on the stiffness values than on the *m*-value. The impact of examined anti-icer mixtures on the creep stiffness of the asphalt binder can be due to the binder emulsification phenomenon (Shi et al. 2009).

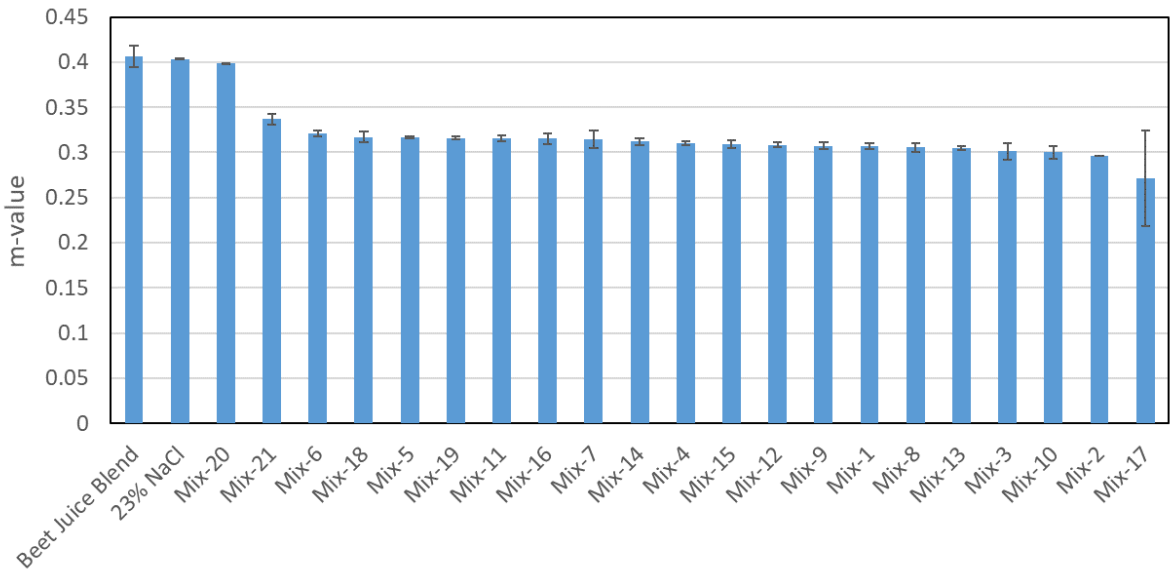

Figure 3.4 The stiffness of asphalt binder exposed to various anti-icer mixtures obtained by a BBR (error bars represent standard error)

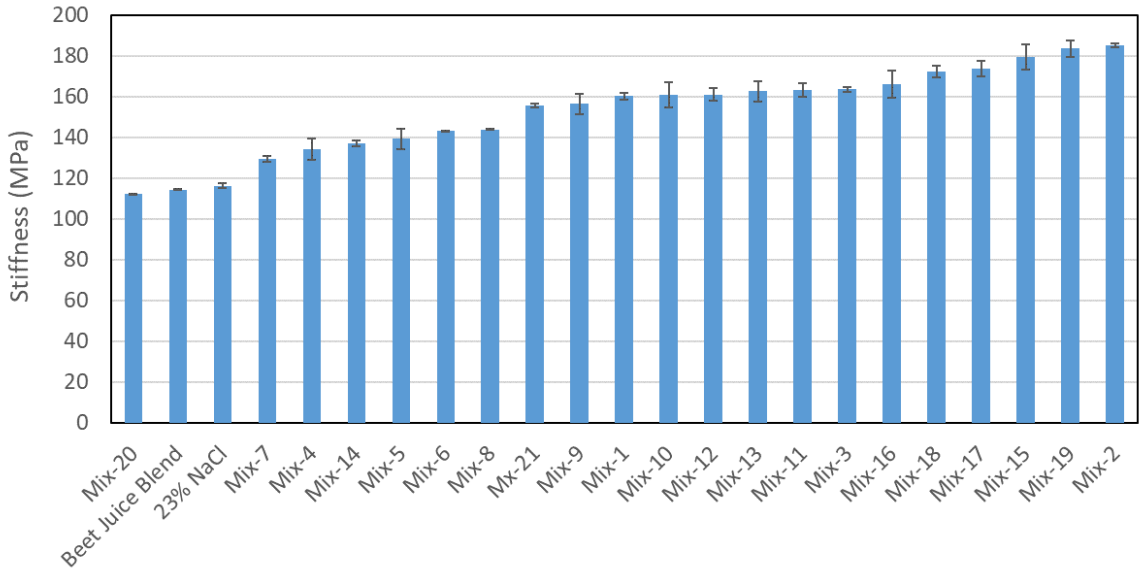

Figure 3.5 The *m*-value of asphalt binder exposed to various anti-icer mixtures obtained by a BBR (error bars represent standard error)

3.4 The Corrosivity of Anti-Icer Mixtures on Mild Steel

As shown in Figure 3.6, the corrosion rates of most of C1010 carbon steel samples exposed to anti-icer mixtures were lower than the corrosion rates of the samples exposed to 23% NaCl brine and beet juice blend. The steel samples exposed to mixtures 2, 3, 5, 6, 8, 9–10, 12–15, 17, and 20

showed average corrosion rates lower than 1 mpy. Among them, Mix-15, which had the highest amount of glycerin (4.8%), caused the lowest corrosion rate of the steel samples (0.12 mpy); Mix-16 showed a corrosivity of around 1.5 mpy. Samples exposed to mixtures 1, 7, 11, and 12 had corrosion rates below 3 mpy. Mixtures 4 and 18 had corrosivity of between 3 and 4 mpy. Note that Mix-18, with zero percent sodium formate, caused the most severe corrosion on the coupons. This result shows the critical role of sodium formate in mitigating general corrosion. Some researchers have shown that formate compounds have a corrosion inhibitory effect on metals (Singh and Singh 1993).

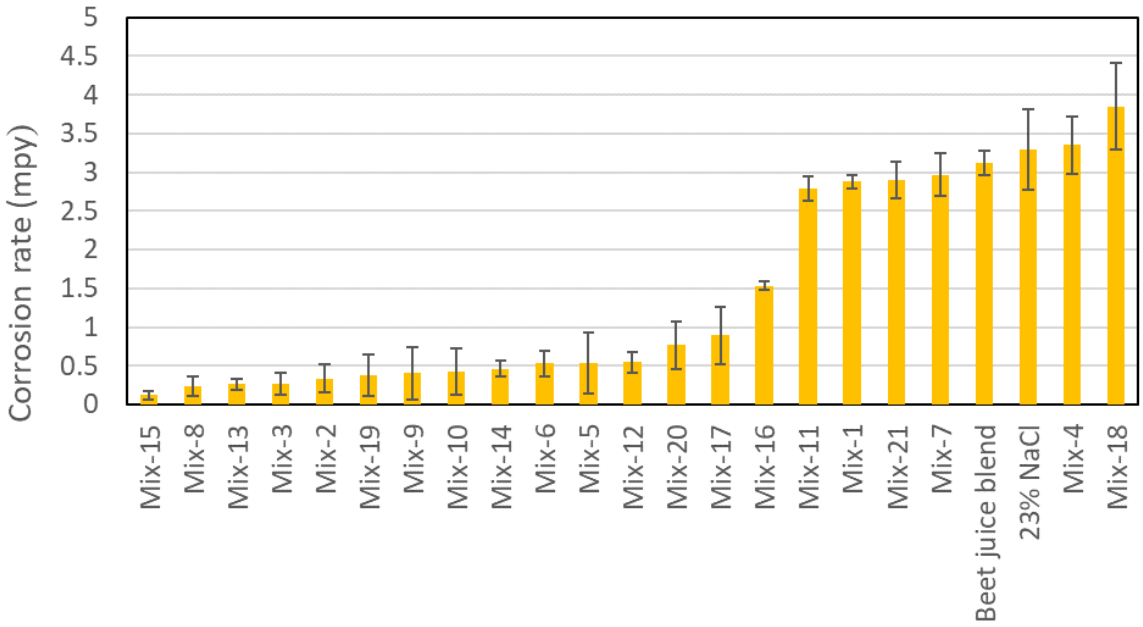

Figure 3.6 Corrosion rates of C1010 carbon steel coupons measured by LPR technique after 24 h immersion in different anti-icer mixtures (error bars represent standard error)

An interesting point is that mixtures 10 and 20, which had the best ice-melting capacity, provided inhibition efficiencies of 92.3% and 86.1%, respectively (calculated using the following equation).

$$IE\% = \left(\frac{CR_{uninhibited} - CR_{inhibited}}{CR_{uninhibited}}\right) \times 100 \qquad (3.1)$$

where *IE* is inhibition efficiency, and $CR_{uninhibited}$ and $CR_{inhibited}$ are the corrosion rates of the steel samples exposed to salt brine and to anti-icer mixtures, respectively.

3.5 Decision-Making Process

The analytical hierarchy process (AHP) was employed for making a decision matrix to prioritize the anti-icer solutions. This process, which assisted us in the multi-criteria decision-making process, allows agencies to evaluate various alternatives in terms of a set of given criteria. Pairwise comparisons, shown in Table 3.1, are made based on the fact that, if the row parameter is considered more important than the parameter in the column, a number greater than one is assigned to the matrix based on the intensity of importance. A higher number indicates greater importance. Conversely, if the parameter in the column is considered more important, the reciprocal of the nonzero value is assigned in the matrix (Triantaphyllou and Mann 1995).

Table 3.1 Pairwise comparisons based on multiple criteria

Comparison	**Ice-melting capacity at 20 min, -3.9°C (25°F)**	**Ice-melting capacity at 60 min, -3.9°C (25°F)**	**Corrosion rate**	**PCM splitting strength**	**Asphalt stiffness**	**Asphalt *m*-value**
Ice-melting capacity at 20 min, -3.9°C (25°F)	1.00	1.00	5.00	1.00	9.00	9.00
Ice-melting capacity at 60 min, -3.9°C (25°F)	1.00	1.00	5.00	1.00	9.00	9.00
Corrosion rate	0.20	0.20	1.00	1.00	2.00	2.00
PCM splitting strength	1.00	1.00	0.11	1.00	2.00	2.00
Asphalt stiffness	0.11	0.11	0.50	0.50	1.00	1.00
Asphalt *m*-value	0.11	0.11	0.50	0.50	1.00	1.00
Sum	3.42	3.42	12.11	5.00	24.00	24.00

The comparisons are used in a standardized matrix to determine the weights of importance of the decision criteria, as shown in Table 3.2. The standardized matrix is the result of the assigned value from Table 3.1 divided by the sum of the assigned values in the respective columns. For example, the 1.00 from row 2 column 2 in Table 3.1 divided by the sum of 3.42 in row 8 column 2 of Table 3.1 gives us 0.29 in row 2 column 2 of Table 3.2. A summary of the prioritization matrix is shown in Table 3.3, in which each column has been normalized, with 0 and 100 being the worst and best performer, respectively. Each decision weight in Table 3.3 was determined by calculating the average of the standardized rows in Table 3.2. For example, from row 1, the average of 0.29, 0.29, 0.41, 0.20, 0.38, and 0.38 is equal to 0.325.

Table 3.2 A standard matrix based on comparisons

Comparison	**Ice-melting capacity at 20 min, -3.9°C (25°F)**	**Ice-melting capacity at 60 min, -3.9°C (25°F)**	**Corrosion rate**	**PCM splitting strength**	**Asphalt stiffness**	**Asphalt m-value**
Ice-melting capacity at 20 min, -3.9°C (25°F)	0.29	0.29	0.41	0.20	0.38	0.38
Ice-melting capacity at 60 min, -3.9°C (25°F)	0.29	0.29	0.41	0.20	0.38	0.38
Corrosion rate	0.06	0.06	0.08	0.20	0.08	0.08
PCM splitting strength	0.29	0.29	0.01	0.20	0.08	0.08
Asphalt stiffness	0.03	0.03	0.04	0.10	0.04	0.04
Asphalt m-value	0.03	0.03	0.04	0.10	0.04	0.04
Sum	1.00	1.00	1.00	1.00	1.00	1.00

Based on the priorities set in Table 3.3, the multi-criteria scoring matrix resulted in Mix-21 having the lowest score (18). Note that five mixtures featured a higher score than 23% NaCl brine control (62) under the investigated conditions and given priorities. Specifically, Mix-10

exhibited the highest score: 81, which is equal to the score of beet juice blend. In the next step, the obtained scores and anti-icer mixtures listed in Table 2.1 were used as inputs in Design-Expert® software to obtain the best-performer sample based on the central composite design method. The best-performer sample contained 0.89% Concord grape extract, 4.57% glycerin, 4.54% sodium formate, 0.19% sodium metasilicate, and 18.4% NaCl.

Table 3.3 Summary of the prioritization

	Weight						
	0.325	**0.325**	**0.094**	**0.160**	**0.048**	**0.048**	
Sample	**Ice-melting capacity at 20 min, -3.9°C (25°F)**	**Ice-melting capacity at 60 min, -3.9°C (25°F)**	**Corrosion rate**	**Splitting strength**	**Asphalt stiffness**	**Asphalt *m*-value**	**Score**
Mix 1	65.22	79.04	26.13	57.61	34.13	0.00	60
Mix 2	70.05	46.08	94.23	25.52	0.00	3.47	51
Mix 3	76.87	64.71	95.95	45.23	29.41	3.80	64
Mix 4	51.51	45.10	13.32	36.89	69.67	4.14	42
Mix 5	71.07	64.71	89.02	43.89	62.80	8.12	63
Mix 6	53.33	49.02	89.10	45.06	57.71	10.04	52
Mix 7	41.97	69.61	23.66	37.15	76.53	13.20	49
Mix 8	25.24	18.63	96.89	34.34	56.62	14.27	32
Mix 9	20.23	40.20	92.45	71.31	39.43	16.23	42
Mix 10	92.79	100.00	91.86	48.04	33.38	16.30	81
Mix 11	45.86	44.12	28.47	56.31	29.98	20.65	43
Mix 12	27.18	46.08	88.59	64.00	33.16	21.02	45
Mix 13	22.06	32.35	96.24	55.33	30.91	21.66	38
Mix 14	58.80	36.27	90.88	36.81	65.74	22.30	50
Mix 15	66.07	41.18	100.00	73.63	7.98	22.40	57
Mix 16	66.92	74.51	61.97	54.41	25.83	25.35	63
Mix 17	16.66	0.00	79.41	60.99	15.77	7.45	24
Mix 18	19.20	22.55	0.00	30.20	17.67	13.57	20
Mix 19	51.18	76.47	93.09	37.42	2.13	10.79	57
Mix 20	100.00	65.69	82.63	50.31	100.00	93.43	79
Mix 21	0.00	41.18	25.49	0.00	40.23	13.48	18
23% NaCl	74.38	68.92	15.02	29.29	94.42	100.00	62
Beet juice blend	78.14	88.22	19.72	100.00	96.95	100.00	81

3.6 Characteristic Temperature

The warming cycle DSC thermogram was used for studying the anti-icers (Figure 3.7), because the warming cycle is less affected by the super-cooling effect and is thus more reliable than the cooling cycle thermogram. Six samples plus BP-4 aged were examined; their composition is shown in Table 3.4.

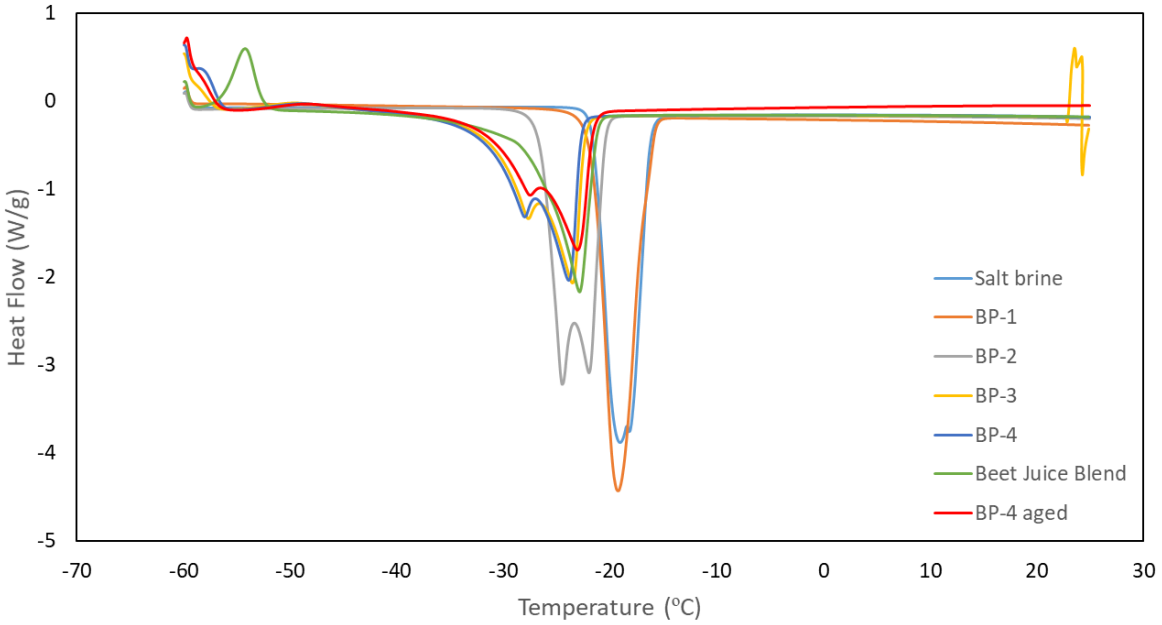

Figure 3.7 DSC thermogram of different deicers; warming cycle

Table 3.4 Composition of different deicers used to obtain DSC thermograms

	Weight% in DI water-based solution				
	Concord grape extract	**Glycerin**	**HCOONa**	**Na_2SiO_3**	**NaCl**
Salt brine					23
BP-1				0.19	18.4
BP-2			4.54	0.19	18.4
BP-3		4.57	4.54	0.19	18.4
BP-4	0.89	4.57	4.54	0.19	18.4
Beet Juice Blend	80% (v/v) 23% NaCl solution + 20% (v/v) beet juice				

For salt brine, at around -18.5°C (-1.3°F), a drop in heat flow between the sample and air (see Fig. 3.7) occurred, which corresponds to the phase transition from ice to water. The temperature associated with the lowest (peak) heat flow (-18.4°C, -1.1°F) is defined as the

characteristic temperature (T_C) of the salt brine sample. The T_C peak relates to the initiation and growth of ice crystals in the test solution. Different chemical solutions would feature thermograms with peaks of unique shape with different values of T_C, which is the basis for using a DSC thermogram as the "fingerprint" of the chemical solutions being tested. Tc coincides with the "effective temperature" of the test solution as a deicer, at which temperature ice crystals start to form and the pavement becomes icy.

By adding 0.19 wt.% sodium metasilicate (Na_2SiO_3) in sample BP-1, the T_C shifted to -19.2°C (-2.6°F). Sample BP-2 had a T_C of around -22°C (-7.6°F), which showed an almost 2.8°C (3°F) decrease in the characteristic temperature due to the addition of 4.54 wt.% sodium formate (HCOONa) to the deicer. Adding 4.57 wt.% glycerin moved the T_C to -23.5°C (-10.3°F). Since nearly the same amount of sodium formate and glycerin were used, it can be concluded that sodium formate is a more effective freezing point depressant than glycerin in the examined deicer. Sample BP-4 had a T_C of -23.9°C (-11°F), which was close to that of Sample BP-3. Therefore, adding 0.89 wt.% Concord grape extract made a minor improvement in the T_C. The T_C of the best-performer sample (BP-4) was less than that of the beet juice blend, with a T_C of -22.8°C (-9°F). In addition, the characteristic temperature of BP-4 aged sample was about -23.1°C (-9.6°F) which is very close to that of BP-4. This shows that aging has not affected the behavior of the BP-4 sample. It should be mentioned that the aging process is performed at 59°C for 3 days (72h) which simulates one-year storage at 24°C (the temperature inside our lab cabinet).

3.7 Complementary Tests

In the complementary tests, the effect of BP-1, BP-2, BP-3, BP-4, and BP-4 aged anti-icers on the following properties were studied.

- Ice melting capacity at 25°F after 20 and 60 min

- Splitting strength of PCM after a 10-cycle freeze-thaw test
- Low temperature behavior of asphalt binder
- Corrosion rate of mild steel

The results are shown in Figures 3.8 to Figure 3.11 show that BP-4 has the best ice melting capacities and anti-corrosion performance, the least impact on PCM samples, and a moderate impact of low temperature performance of asphalt binder. In addition, aging of BP-4 had a a negligible impact on the ice melting capacity, PCM strength after 10 cycles of freeze-thaw, and low temperature stiffness of asphalt binder. Therefore, it can be concluded that aging has a minor impact on the key properties of best performer sample.

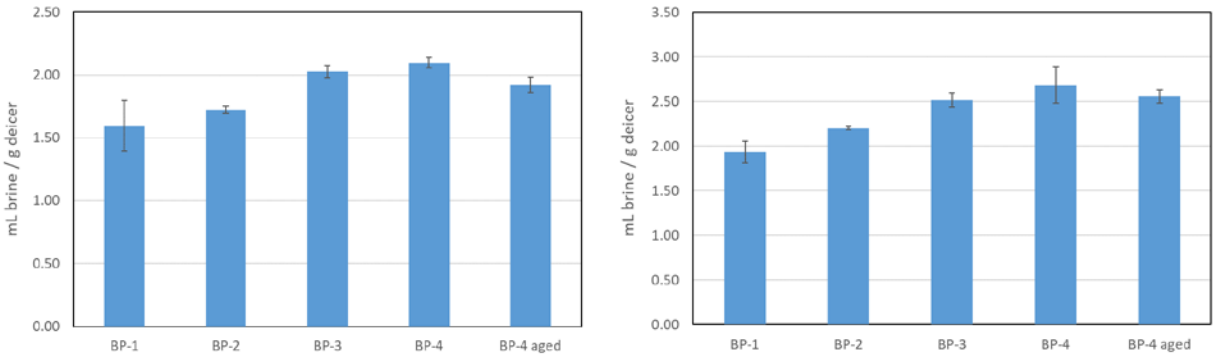

Figure 3.8 Ranking of mixtures based on ice-melting capacity after application of anti-icers at 20 min (left) and 60 min (right), and 25°F obtained using a SHRP test method (error bars represent standard error)

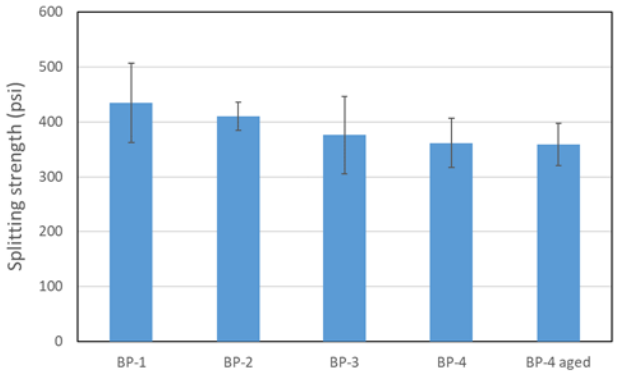

Figure 3.9 Splitting strength of mortar as a function of anti-icer type after 10-cycle freeze-thaw test (error bars represent standard error)

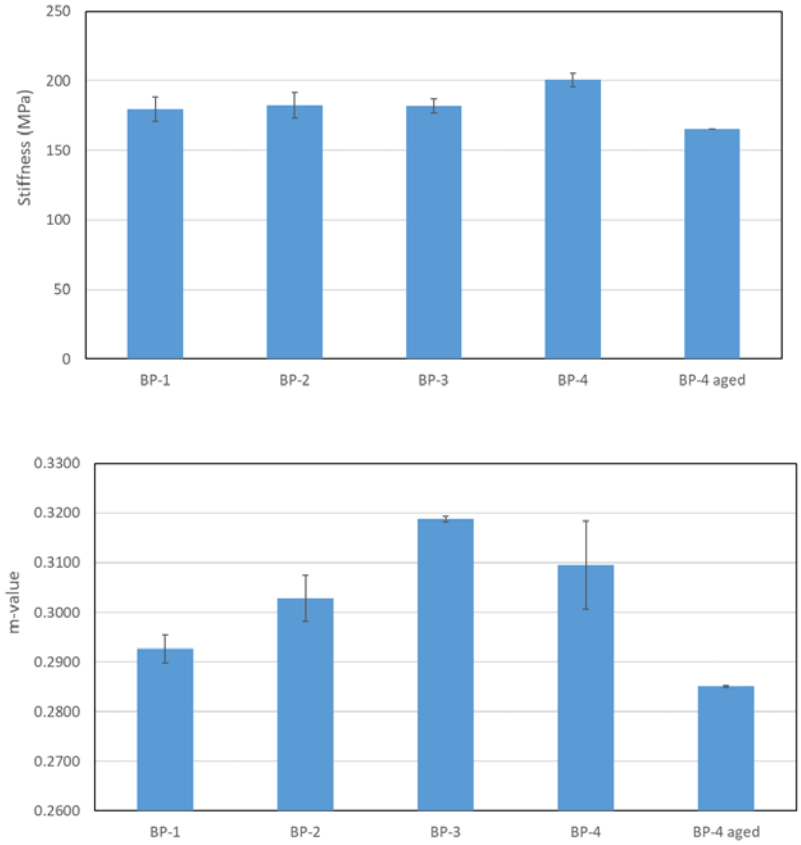

Figure 3.10 The stiffness (above) and *m*-value of asphalt binder exposed to various anti-icer mixtures obtained by a BBR (error bars represent standard error)

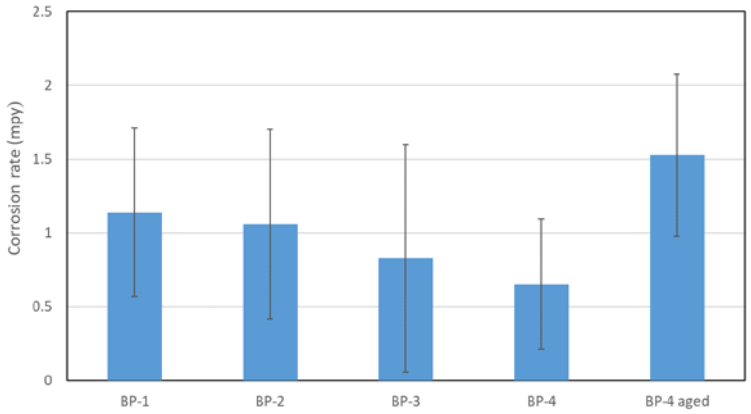

Figure 3.11 Corrosion rates of C1010 carbon steel coupons measured by LPR technique after 24 h immersion in different anti-icer mixtures (error bars represent standard error)

3.8 Chemical Oxygen Demand

The mg/L COD (chemical oxygen demand) data reflect measures of milligrams of oxygen consumed per liter of sample via the standard procedure mentioned earlier. In measuring the mg/L COD, both solutions were diluted to a ratio of 1000:1 by adding DI (deionized) water. For measuring the pH, original solutions were used. The associated data are presented in Table 3.5, which shows that the best-performer sample has almost half the COD of the beet juice blend. However, the pH of the best-performer sample is twice that of the beet juice blend. By increasing the pH value, the COD removal efficiency increases in wastewater systems (Sivrioğlu and Yonar 2015). In fact, in the alkaline condition, a high concentration of OH^- ions can provide oxygen necessary for oxidation of chemicals and can decrease the need for external oxygen.

Table 3.5 Chemical oxygen demand and pH of best-performer sample and beet juice blend

Sample	mg/L COD	pH
Beet juice blend	277.94	5.3
Best performer	135.17	11.7

3.9 Snow–Pavement Bond and Friction Measurements

Figure 3.12 shows the effect on the friction coefficient of asphalt concrete when different deicers are applied. Surprisingly, no improvement of the friction coefficient was observed by deicing (pre-wet salt). Similar results were observed by Akin et al. (2018) on ultrathin friction course new (< 2 years) and open-graded friction course old (> 4 years) pavement types. On the other hand, a considerable decrease in snow–pavement bond shear strength was observed when beet juice blend and BP-3 solution were used for anti-icing (Figure 3.13).

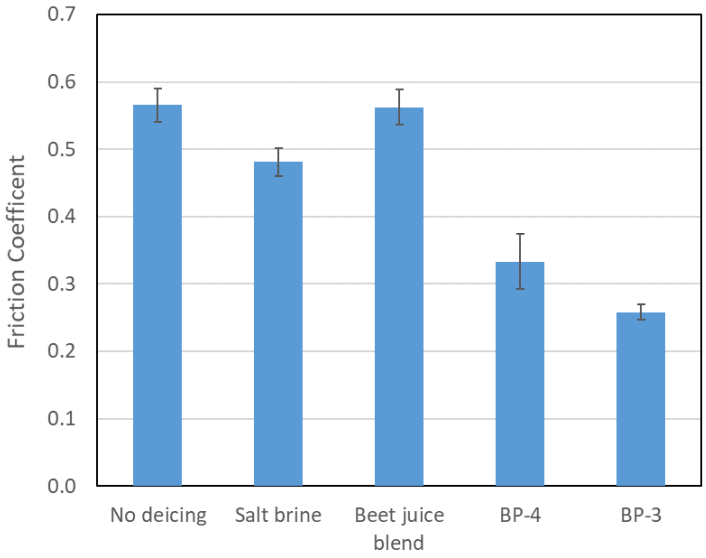

Figure 3.12 Friction coefficient after plowing at 25°F in the absence of deicer and after deicing by salt brine, beet juice blend, BP-4, and BP-3

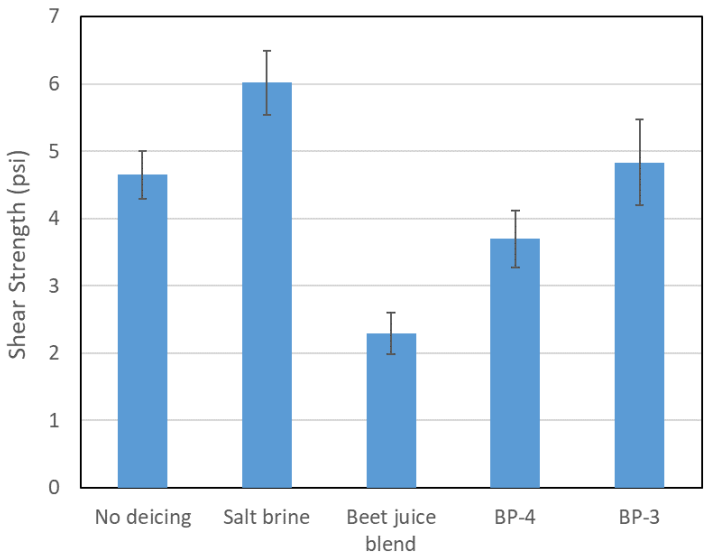

Figure 3.13 Snow-pavement bond test results at 25°F in the absence of deicer and after deicing by salt brine, beet juice blend, BP-4, and BP-3

The effect on the friction coefficient of asphalt concrete after applying different anti-icers is seen in Figure 3.14, which shows that anti-icing has decreased the friction coefficient of asphalt pavement. These results are in contradiction with our previous research, which showed a benefit

of anti-icing on the friction coefficient of asphalt concrete. Therefore, we conclude that the effect on the friction coefficient of using anti-icers depends highly on pavement type.

Akin et al. (2018) showed that asphalt pavement type affects the efficiency of the anti-icing process, which is in good agreement with our findings. Figure 3.15 depicts snow–pavement bond shear strength in case of no anti-icing and anti-icing using salt brine, beet juice blend, and BP-4 and BP-3 anti-icers. All of the anti-icers decreased shear strength, which demonstrates that their use can facilitate the plowing process.

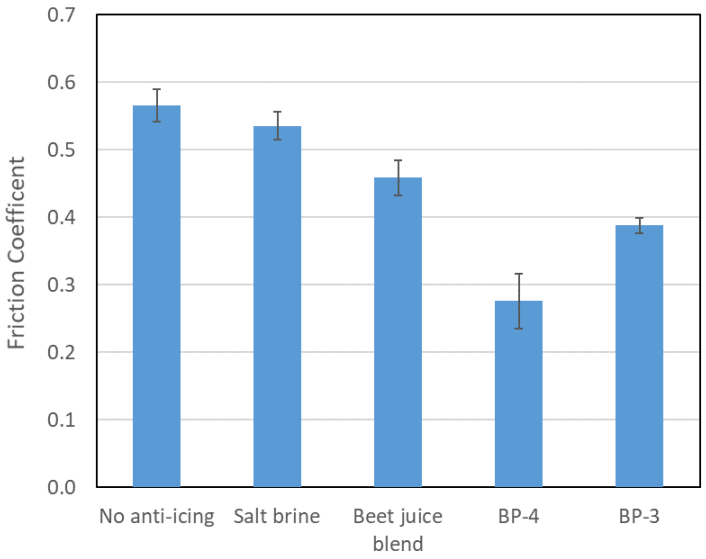

Figure 3.14 Friction coefficient after plowing at 25°F in the absence of anti-icer and after anti-icing by salt brine, beet juice blend, BP-4, and BP-3

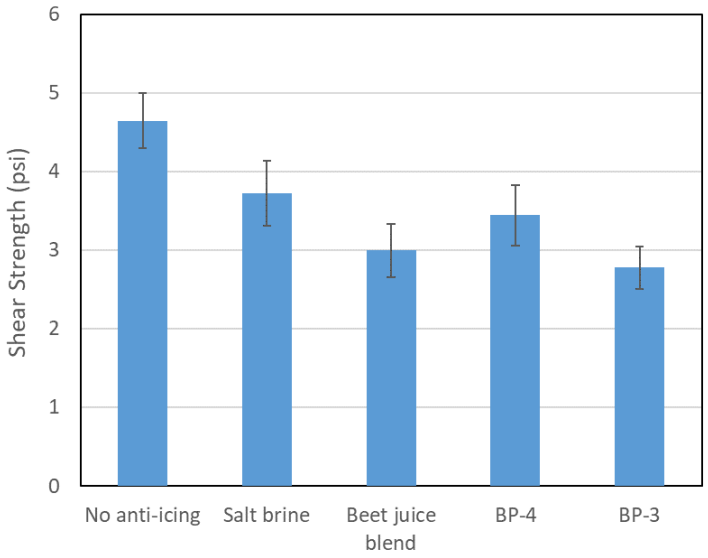

Figure 3.15 Snow-pavement bond test results at 25°F in the absence of anti-icer and after anti-icing by salt brine, beet juice blend, BP-4, and BP-3

CHAPTER 4.0 CONCLUSIONS

This report describes the performance and impacts of 21 anti-icer mixtures that were designed using the central composite design method based on the preliminary experiments of the authors. Selected constituent materials pose minimal toxicity to the environment (e.g., no heavy metal content) and were derived from eco-friendly, cost-effective processes. Agro-based solutions derived from locally sourced agro-based materials mixed with salt brine, and commercial additives (with little toxicity) were tested for their ice-melting capacity, ice-penetration rate, ability to protect asphalt binder and concrete, effect on the friction coefficient of deiced and anti-iced asphalt pavement, and anti-corrosion performance. The main criterion for choosing the best-performing anti-icer was ice-melting capacity. A decision-making process based on an analytical hierarchy process (AHP) was used to determine the best-performing anti-icer. The best-performer anti-icer mixture contained 0.89% Concord grape extract, 4.57% glycerin, 4.54% sodium formate, 0.19% sodium metasilicate, 18.4% NaCl, and water. This mixture was an alkaline solution with half of the chemical oxygen demand of traditional beet juice blend. Differential scanning calorimetry thermograms showed the critical role of glycerin and sodium formate in the relatively low critical temperature of this mixture (-11°F) and the mixture's superiority over sugar beet blend and salt brine. In addition, aging of best performer sample had a minor impact on the key properties of best performer sample. A considerable decrease in the snow–pavement bond shear strength was observed when the best-performer solution was used for anti-icing. Friction tests showed that the effect of deicing and anti-icing on the friction coefficient is highly dependent on pavement type.

References

Akin, M., Cuelho, E., Fay, L., Muthumani, A., 2018. Winter Maintenance, Friction and Snow–Pavement Bond on Permeable Friction Surfaces (Final Report). Minnesota Department of Transportation.

Bloomer, T.A., 2002. Anti-freezing and deicing composition and method. US6416684 B1.

Chappelow, C.C., McElroy, A.D., Blackburn, R.R., Darwin, D., Locke, C.E., 1992. Handbook of Test Methods for Evaluating C h emical Deicers. Strategic Highway Research Program, National Research Council, National Academy of Sciences, Washington D.C.

Conger, S.M., 2005. Winter Highway Operations, NCHRP Synthesis 344. Transportation Research Board, Washington, DC.

Fay, L., Jungwirth, S., Li, Y., Shi, X., 2014. Toxicological Effects of Chloride-Based Deicers in the Natural Environment: Synthesis of Existing Research - Transport Research International Documentation - TRID. Presented at the Transportation Research Board 93rd Annual Meeting, Washington, DC.

Fay, L., Shi, X., Huang, J., 2013. Strategies to Mitigate the Impacts of Chloride Roadway Deicers on the Natural Environment, NCHRP Synthesis 449. Transportation Research Board, Washington, DC.

Johnson, A.R., 2017. Methods fluids by producing and employing oil and gas well drilling and completion fluids as well as hydraulic fracturing fluids employing triglyceride processing by products and propylene glycol recovered from aircraft deicing operations. US9725641B2.

Li, Y., Fang, Y., Seeley, N., Jungwirth, S., Jackson, E., Shi, X., 2013. Corrosion by Chloride Deicers on Highway Maintenance Equipment: Renewed Perspective and Laboratory Investigation. Transp. Res. Rec. J. Transp. Res. Board 2361, 106–113. https://doi.org/10.3141/2361-13

Lilek, J., 2017. Roadway deicing in the United States [WWW Document]. Am. Geosci. Inst. URL https://www.americangeosciences.org/critical-issues/factsheet/roadway-deicing-united-states (accessed 6.9.18).

Metal Samples, 2018. Introduction to Linear Polarization Resistance (LPR) Monitoring [WWW Document]. URL http://www.alspi.com/lprintro.htm (accessed 5.10.18).

Ossian, K.C., Behrens, K., 2009. Processed raffinate material for enhancing melt value of de-icers. US7473379 B2.

Sapienza, R., Johnson, A., Ricks, W., 2012. Environmentally benign anti-icing or deicing fluids. US8241520B2.

Shi, X., Akin, M., Pan, T., Fay, L., Liu, Y., Yang, Z., 2009. Deicer Impacts on Pavement Materials: Introduction and Recent Developments. Open Civ. Eng. J. 3, 16–27.

Shi, X., Veneziano, D., Xie, N., Gong, J., 2013. Use of chloride-based ice control products for sustainable winter maintenance: A balanced perspective. Cold Reg. Sci. Technol. 86, 104–112. https://doi.org/10.1016/j.coldregions.2012.11.001

Simmons, K.L., Jr, J.G.F., Werpy, T.A., Samuels, W.D., Conkle, H.N., Monzyk, B.F., Kuczek, S.F., Chauhan, S.P., 2007. Biobased deicing/anti-icing fluids. US7169321B2.

Singh, R.N., Singh, V.B., 1993. Corrosion Behavior and Inhibitive Effects of Organotin Compounds on Nickel in Formic Acid. CORROSION 49, 569–575. https://doi.org/10.5006/1.3316086

Sivrioğlu, Ö., Yonar, T., 2015. Determination of the acute toxicities of physicochemical pretreatment and advanced oxidation processes applied to dairy effluents on activated sludge. J. Dairy Sci. 98, 2337–2344. https://doi.org/10.3168/jds.2014-8278

Staples, J.M., Gamradt, L., Stein, O., Shi, X., 2004. Recommendation for Winter Traction Materials Management on Roadways Adjacent to Bodies of Water (No. FHWA/MT-04-008/8117-19). Montana Department of Transportation, Helena, MT.

Taylor, P., Verkade, J., Gopalakrishnan, K., Wadhwa, K., Kim, S., 2010. Development of an Improved Agricultural-Based Deicing Product (Final Report No. IHRB Project TR-581). Institute for Transportation, Iowa State University.

Triantaphyllou, E., Mann, S.H., 1995. Using the analytic hierarchy process for decision making in engineering applications: Some challenges. Int. J. Ind. Eng. 2.

Ye, Z., Strong, C., Fay, L., Shi, X., 2009. Cost Benefits of Weather Information for Winter Road Maintenance, Final Report for the Aurora Consortium led by the Iowa Department of Transportation.